Monthly Notices
of the
ROYAL ASTRONOMICAL SOCIETY

Mon. Not. R. Astron. Soc. **401,** 1850–1856 (2010) doi:10.1111/j.1365-2966.2009.15761.x

Two new variable sdB stars, HE 0218−3437 and LB 1516

C. Koen,[1⋆] D. Kilkenny,[2] M. L. Pretorius[3,4] and D. J. Frew[5,6]

[1]*Department of Statistics, University of the Western Cape, Private Bag X17, Bellville 7535, South Africa*
[2]*Department of Physics, University of the Western Cape, Private Bag X17, Bellville 7535, South Africa*
[3]*South African Astronomical Observatory, PO Box 9, Observatory 7935, South Africa*
[4]*European Southern Observatory, Alonso de Cordova 3107, Santiago, Chile*
[5]*Perth Observatory, 337 Walnut Road, Bickley, WA 6076, Australia*
[6]*Department of Physics, Macquarie University, NSW 2109, Australia*

Accepted 2009 September 21. Received 2009 September 15; in original form 2009 August 18

ABSTRACT

We present photometry which shows that two known hot subdwarf stars, HE 0218−3437 and LB 1516, are variable. LB 1516 exhibits several frequencies in the range 12–25 cycles d^{-1} (periods of about 1–2 h) with amplitudes less than about 0.003 mag and appears to be a typical slowly pulsating sdB star. Results from a multisite campaign on HE 0218−3437 show the presence of two frequencies only, the lower amplitude variation an apparent subharmonic of the higher amplitude periodicity. It is likely that the star is in a binary system, and that the variability is due to ellipsoidal deformation of the primary star.

Key words: stars: individual (HE 0218−3437; LB 1516) – stars: oscillations – stars: variables: other.

1 INTRODUCTION

A little more than a decade ago, the first pulsating sdB stars were discovered (Kilkenny et al. 1997) – almost simultaneously with, but independently of, the prediction that such stars should pulsate (Charpinet et al. 1996). These V361 Hya stars have very short periods (typically ∼2 to 5 min); they normally have several oscillation frequencies (in some cases, over 40 frequencies have been detected); they have surface temperatures around $28\,000 < T_{\rm eff} < 35\,000$ K and surface gravities $5.2 < \log g < 6.1$; and they are believed to be *p*-mode oscillators. More recently, a separate, somewhat cooler group of *slowly* pulsating sdB stars has been discovered by Green et al. (2003). These V1093 Her stars are usually multiperiodic variables with periods of the order of one to two hours and are probably *g*–mode pulsators. Additionally, three fascinating stars have very recently been found to exhibit *both p*- and *g*-mode variations (see e.g. Oreiro et al. 2004; Schuh et al. 2006; Lutz et al. 2009).

The pulsating sdB stars provide potential for examining the internal structure of hot subdwarfs via identification of pulsation modes (see Van Grootel et al. 2008b; Charpinet et al. 2008, for recent examples), and for the determination of the rate of evolution via secular frequency changes caused by radius/mean density changes. The discovery of new variables is desirable to extend the sample of stars for such analyses; to test the existence of an 'instability strip' or preferred temperature zone for pulsation; and to test the detected frequencies against pulsation models. Recent reviews of the observational and theoretical work on pulsating sdB stars have been given by Kilkenny (2007) and Charpinet et al. (2007), respectively.

In this paper, we present results which show two known hot subdwarf stars to be variable. Both were selected as target slowly pulsating sdB stars, based on their relatively cool temperatures (Table 1). The star LB 1516 is from 'A search for faint blue stars' by Luyten & Anderson (1958). The second star, HE 0218−3437, is an sdB star found by the Hamburg/European Southern Observatory (ESO) survey (see e.g. Altmann, Edelmann & de Boer 2004). Some fundamental quantities of the two stars are listed in Table 1.

The first star does indeed show pulsations, but, as will be shown below, the origin of the variability in HE 0218−3437 is less obvious.

2 HE 0218−3437

There is apparently very little published material available for HE 0218−3437. It was included in the kinematic study by Altmann et al. (2004) who give *BVR* photometry as well as *Hipparcos* proper motions and a parallax ($d = 0.81$ kpc) and their own measure of radial velocity (+38 km s^{-1}). Ortiz et al. (2007) also classified the star sdB in their spectroscopic survey of blue Two Micron All Sky Survey (2MASS) stars near the south Galactic pole; they detected no He I lines.

2.1 Discovery observations

Observations made in 2008 October showed this star to be a small-amplitude variable with a period near 4000 s and an amplitude ∼0.01 mag. The discovery data were single-filter (V) and were obtained with the South African Astronomical Observatory (SAAO) STE4

⋆E-mail: ckoen@uwc.ac.za

Table 1. New slowly pulsating sdB star candidates.

Star	HE 0218–3437	LB 1516
V	13.39	12.97
$(B-V)$	−0.25	−0.25
$(U-B)$		−0.93
$T_{\rm eff}$	25 300	26 100
$\log g$	5.4	5.4

Note. Photometry is taken from Landolt (2007) (LB 1516) and Altmann et al. (2004) (HE 0218–3437). The temperature and gravity determinations are from Edelmann (2003): the uncertainties in $T_{\rm eff}$ are 300 and 1500 K, and in $\log g$ 0.1 and 0.2, for HE 0218–3437 and LB 1516, respectively.

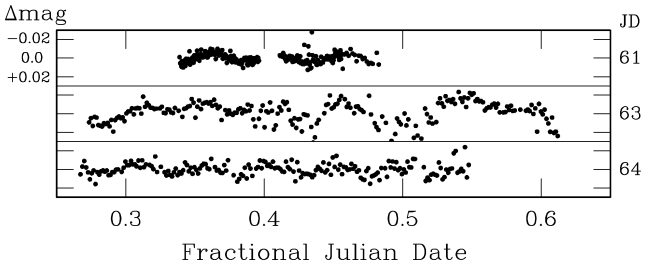

Figure 1. V-band differential observations for HE 0218–3437 from October 2008. The numbers at the right-hand edge of the figure are JD−245 4700 (see Table 2).

CCD camera on 2008 October 21/22. Further *BVI* observations were made with the SAAO 1-m telescope and UCTCCD camera (O'Donoghue 1995) on 2008 October 23/24 and 24/25 which confirmed the variations. The October photometric data are illustrated in Fig. 1.

This discovery proved to be particularly fortuitous, as we had planned a multisite campaign on another sdB star which we had believed to be a slow pulsator with interesting characteristics, but which turned out to be a rapid pulsator (a fluke of aliasing!). This target was then entirely unsuitable for a campaign involving conventional-readout CCDs which would not give the required resolution in time. Thus, at the last minute, HE 0218−3437 was substituted as the target for the campaign, the results from which form the bulk of the data reported here.

2.2 The multisite campaign

Observations obtained at Perth Observatory, Bickley, Western Australia, used the 61-cm Perth-Lowell telescope. *B*, *V* and *I* images were recorded with an Apogee AP7 camera using a SITe 512 × 512 back-illuminated chip with 24-μm pixels. The field of view is 300 arcsec^2 at a plate scale of 0.58 arcsec pixel^{-1}. No on-chip binning was used, and the exposure times were 90 s in *B*, 60 s in *V* and 60–90 s in *I*, using standard Bessell filters. The exposure times were relatively long to compensate for the smaller aperture of the telescope. Readout time was ∼15 s. The CCD images were reduced using standard techniques which included bias and flat-field corrections. The photometric reductions were done using point-spread function (PSF) fitting using a modified version of the DOPHOT package (Schechter, Mateo & Saha 1993), with the flux of the target star differentially compared to three comparison stars in the field.

Observations at Cerro Tololo Inter-American Observatory (CTIO) in Chile were obtained with the Yale 1-m telescope administered by the Small and Moderate Aperture Research Telescope System (SMARTS) consortium. The dedicated instrument is the Y4KCam, a 4064 × 4064 CCD with a 400 arcsec^2 field of view and a pixel scale of 0.29 arcsec pixel^{-1}. The CCD was operated in unbinned mode throughout. Exposure times were 50–70 s in *B*, 30–50 s in *V* and 30–50 s in *I*. Although the readout and file writing time was of the order of 70 s, the duty cycle was still sufficiently short to clearly delineate the brightness variations. Bias subtraction, as well as flat-field and illumination corrections, were performed with IRAF scripts kindly provided by Dr. Phil Massey (Lowell Observatory). Since stellar image properties varied across the field of view, the frames were then trimmed to include images of only HE 0218−3427 and half a dozen or so bright local comparison stars. Aperture photometry was performed on these objects using DOPHOT.

The SAAO observations were made using the Sutherland 1-m telescope and STE3 camera, which uses a SITe 512 × 512 CCD having about 160 arcsec^2 field of view and a scale of 0.31 arcsec pixel^{-1}. The CCD was operated in unbinned mode and typical exposures were 60 s in *B* and 40 s in *V* and *I*. Only about 16 s were lost between each exposure for CCD readout and filter change. Reductions were performed much as for the CTIO data, except that the full field reduction only included two local 'comparison' stars as well as the target, because of the much smaller CCD.

Photometry of HE 0218−3437 from each site was corrected differentially on a night-by-night basis to remove any rapid transparency variations using nearby bright stars. In general, this meant two 'comparison' stars on the SAAO frames, three on the Perth frames and about six on the CTIO frames. Since almost everything in the visible Universe is a K or M star, random field stars will almost always be quite red, and certainly much redder than our target sdB star. We might expect differential extinction effects to be significant, and they appear so in our results. We have therefore further corrected for residual atmospheric extinction effects by removing a quadratic term from each night's observations. As can be seen from Fig. 2, this simple procedure 'flattens' the observations quite successfully.

Table 2 gives a log of the 2008 October and November photometry and Fig. 2 illustrates the *V* results from November. The *B* and *I* results are very similar in appearance to Fig. 2 except that the *I* data are clearly somewhat noisier. Note that the data from all sites are much denser on November 23/24 (JD 245 4794) as only the *V* filter was used on that night (to look – unsuccessfully – for shorter period variations). In all, we have accumulated a little over 64 h of *V* photometry (and about 58.5 h data for each of the *B* and *I* bands). This is about 53 per cent coverage in *V* and ∼49 per cent in *B* and *I*; which is good for a campaign involving only three sites.

2.3 Analysis

The frequency analyses described in this paper were carried out using the EAGLE software written by Darragh O'Donoghue which produces Fourier amplitude spectra following the Fourier transform method of Deeming (1975) as modified by Kurtz (1985).

For at least the first half of the multisite campaign, it appeared that HE 0218−3437 was singly periodic or, at least, that only one frequency could be detected in the periodograms for all three colours. Towards the end of the campaign, as more and more observations were added into the solutions, it became clear that, although very weak, the next highest peak (in the range 0 to 40 cycles d^{-1}) in each of the *V* and *B* sets of photometry had closely similar frequencies. Additionally, this very weak peak in each colour is at almost exactly half the frequency of the very obvious peak and would therefore

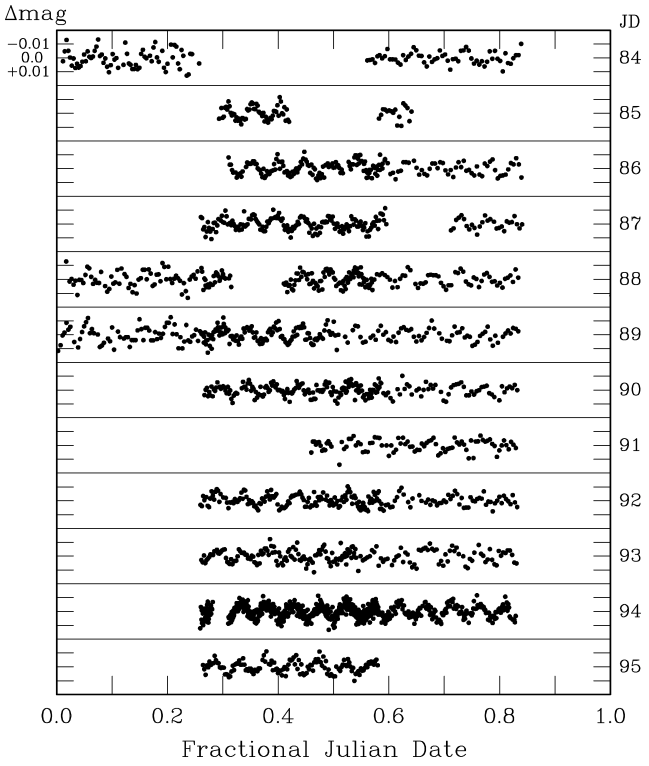

Figure 2. *V*-band differential observations for HE 0218–3437 from 2008 November; the multisite campaign. Numbers at the right-hand edge of the figure are JD−245 4700 (see Table 2). Data to the left are from Perth Observatory; in the centre are from the SAAO; and on the right from Cerro Tololo Inter-American Observatory (CTIO). The SAAO data are somewhat denser as the SAAO STE3 CCD is smaller than those at CTIO and Perth, so the read-out time is substantially smaller. On JD 2454794, only *V* data were obtained, so the density of observation is much higher at all sites.

appear to be the first subharmonic of it. Periodograms for all three sets of photometry are shown in Fig. 3 and the extracted frequencies and amplitudes are listed in Table 3.

In both *B* and *V*, the main peak is near 21.05 d^{-1} (243.6 μHz; 4105 s) and the subharmonic is at 10.53 d^{-1} (121.9 μHz; 8205 s). Although, in both cases, this weak peak is only about three times the background noise, independent detection in both sets of photometry is compelling evidence for them being real. This peak is not unambiguously detected in *I*. There is a peak at 10.52 d^{-1} but it is not the next strongest peak after the main one; it is the third strongest (in the range 0 to 40 cycles d^{-1}) and is therefore really indistinguishable from noise, being only about twice the background. We have included the details for the *I* subharmonic in Table 3, even though it is less convincing than those in *V* and *B*. Fig. 4 shows the analysis of the same observations used in Fig. 3, but pre-whitened by the single strong frequency at 21.05 d^{-1}.

A noteworthy feature of the table is the significant difference between the phase of the principal *I*-band mode, and the corresponding *B* and *V* filter phases. This is easily shown to be due to the significant *frequency* differences: if a sinusoid with $f = 21.050\,d^{-1}$ is fitted to the *I* data, an amplitude of 3.7(2) and phase −0.33(5) are obtained.

As a further step, the underlying light curve shapes giving rise to the amplitude spectra can be extracted directly from the data without too much effort. First the data are folded with respect to the subharmonic frequency, and then smoothed. Graphs obtained by

Table 2. Photometry log for HE 0218–3437.

Date (2008)	Obs.	Duration JD(245 4700+)	Duration (h)	Filters
Oct				
1/22	SAAO	61.339–0.483	3.5	*V*
23/24	SAAO	63.273–0.612	8.1	*BVI*
24/25	SAAO	64.267–0.547	6.7	*BVI*
Nov				
13/14	Perth	84.011–0.257	5.9	*BVI*
	CTIO	84.561–0.839	6.7	*BVI*
14/15	SAAO	85.293–0.420	3.0	*BVI*
	CTIO	85.582–0.641	1.4	*BVI*
15/16	SAAO	86.310–0.592	6.8	*BVI*
	CTIO	86.545–0.839	7.1	*BVI*
16/17	SAAO	87.260–0.595	8.0	*BVI*
	CTIO	87.712–0.841	3.0	*BVI*
17/18	Perth	88.017–0.268	6.0	*BVI*
	SAAO	88.263–0.551	6.9	*BVI*
	CTIO	88.517–0.834	7.6	*BVI*
18/19	Perth	89.002–0.304	7.2	*BVI*
	SAAO	89.261–0.509	6.0	*BVI*
	CTIO	89.521–0.834	7.5	*BVI*
19/20	SAAO	90.267–0.585	7.6	*BVI*
	CTIO	90.513–0.832	7.7	*BVI*
20/21	SAAO	91.460–0.496	0.9	*BVI*
	CTIO	91.510–0.829	7.6	*BVI*
21/22	SAAO	92.260–0.586	7.8	*BVI*
	CTIO	92.521–0.832	7.5	*BVI*
22/23	SAAO	93.261–0.535	6.6	*BVI*
	CTIO	93.513–0.831	7.6	*BVI*
23/24	SAAO	94.259–0.581	7.7	*V*
	CTIO	94.521–0.829	7.4	*V*
24/25	SAAO	95.263–0.580	7.6	*BVI*

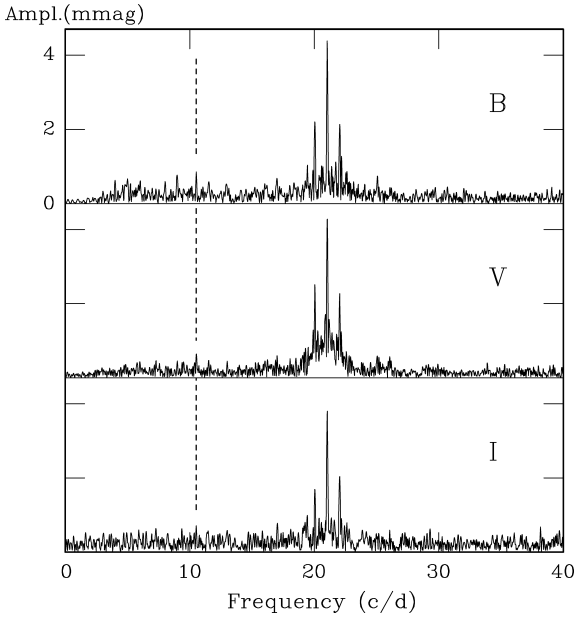

Figure 3. Amplitude spectra of the *V*, *B* and *I* observations for HE 0218–3437, including all the observations from the multisite campaign (see Table 2). In each panel, the general appearance of the spectral window can be inferred from the appearance of the very strong feature near 21.05 d^{-1}. The vertical dashed line is at exactly half that frequency, to draw attention to the subharmonic.

Table 3. Results for the frequency detected in HE 0218–3437 and its subharmonic.

Filter	Frequency (d^{-1})	Amplitude (mmag)	Phase (rad)
B	21.050 (1)	4.4 (1)	−0.33 (3)
	10.531 (7)	0.8 (1)	−2.1 (1)
V	21.049 (1)	4.35 (9)	−0.33 (2)
	10.533 (7)	0.57 (9)	−2.4 (2)
I	21.044 (2)	3.7 (2)	−0.11 (5)
	10.526 (14)	0.6 (2)	−2.4 (3)

Note. Figures in brackets are the uncertainties in the last quoted digit; these are formal errors, which could consistently underestimate the true errors.

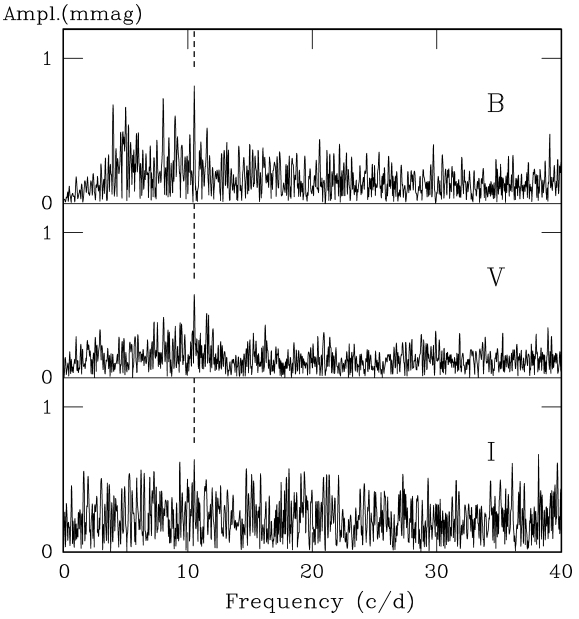

Figure 4. Amplitude spectra of the *V*, *B* and *I* observations for HE 0218–3437, pre-whitened by the single largest peak at 21.05 d^{-1} (see Fig. 3). The vertical dashed line is at exactly half that frequency, to draw attention to the subharmonic near 10.53 d^{-1}.

simple binning are too rough; better results follow from smoothing, but since the data are not uniform in phase, an ordinary running average cannot be used. Instead, we make use of a smoothing method named 'loess' (see e.g. Cleveland 1979; Cleveland & Devlin 1988), which can be applied to irregularly spaced data. The backbone of the method is the fitting of a low order polynomial to short sections of the data, by weighted regression. In the present case, we use second order polynomials, fitted to phase intervals of the order of 0.2. The results for each of the filters are plotted in Fig. 5. The differences in the depths of successive minima are clearly visible in all three cases: these seem more pronounced in *B* and *V*.

2.4 Discussion

The fact that 12 nights of intensive observing uncovered only a single frequency, and its apparent subharmonic, gives pause for thought. Both the light curve shape and the monoperiodicity argue against pulsation as an explanation for the variability. Alternatives involve starspots and/or binarity. Two dark spots of unequal size and/or temperature, symmetrically placed on the stellar surface, could certainly explain the light curves, but raises the question of the spot origin.

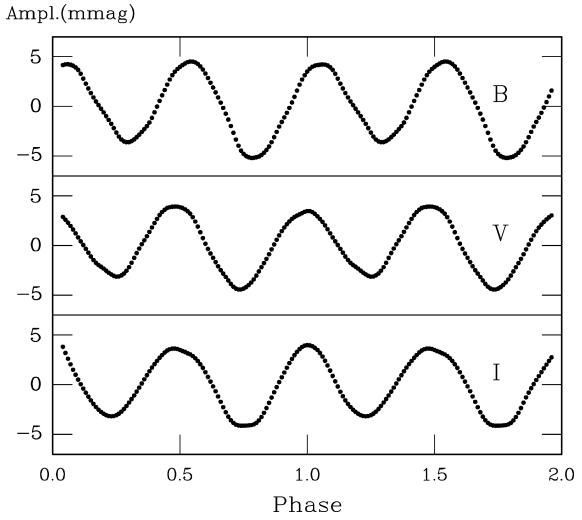

Figure 5. Multisite data for HE 0218–3437, folded on the 'subharmonic' frequency of 10.53 d^{-1} and smoothed using the 'loess' method (Cleveland 1979; Cleveland & Devlin 1988). Note the difference in successive minima in all three colours.

A more plausible explanation is ellipsoidal variability, induced by an unseen binary companion. The likely companion to the sdB star is a compact object, rather than a cool main sequence star (or brown dwarf). This follows since there is no indication of an infrared excess from the 2MASS measurements when the star is placed in colour–colour diagrams as given by Stark & Wade (2003) and Reed & Stiening (2004). More telling, there is no obvious heating of the surface of a cool object.

It is unlikely, though not impossible, that the companion is a neutron star or black hole (see e.g. Geier et al. 2008a). In the absence of a radial velocity study which would hopefully supply a mass function, we proceed with the more likely assumption that the companion is a white dwarf (WD). The list of similar binaries – i.e. short period sdB + WD systems showing ellipsoidal deformation – is short, consisting of KPD 0422+5421 (Koen, Orosz & Wade 1998) and KPD 1930+2752 (Geier et al. 2007). The periods of the two binaries (2.16 and 2.28 h) are remarkably close to that of HE 0218–3437 (2.28 h). Although the masses of the sdB stars in the two previously known systems are very similar (close to 0.5 $M_\odot$), the total binary masses are rather different – 1.04 $M_\odot$ in the case of KPD 0422+5421 (Orosz & Wade 1999), and 1.4–1.5 $M_\odot$ in the case of KPD 1930+2752 (Geier et al. 2007). It follows that KPD 1930+2752 is a possible Type Ia supernova (SN Ia) progenitor, while KPD 0422+5421 is not.

Rotational synchronization of the sdB star with the binary period has been confirmed for KPD 0422+5421 and KPD 1930+2752. In fact, tidal locking has also been observed in the two longer period sdB + WD binaries Feige 48 ($P = 9.02$ h; Van Grootel et al. 2008a) and PG 0101+039 ($P = 13.68$ h; Geier et al. 2008b). It is therefore reasonable to expect the rotation of the sdB star in the HE 0218−3734 system to be synchronous. This is useful, as it would allow the orbital inclination *i* of the binary to be constrained from measurements of $v \sin i$ (e.g. Geier et al. 2008b).

The generally accepted explanation for the origin of sdB + WD systems is common envelope ejection (e.g. Han et al. 2003). Population synthesis studies then suggest a mass of the subdwarf star in the range 0.30–0.48 $M_\odot$, with a peak near 0.47 $M_\odot$ (Han et al. 2002). This information, together with measured $v \sin i$ and the

mass function

$$f = \frac{M_{\rm WD}^3 \sin^3 i}{(M_{\rm WD} + M_{\rm sdB})^2} ,$$

could then be used to constrain the mass of the WD star.

The estimated properties of the sdB stars in KPD 0422+5421 and HE 0218−3734 are quite similar: effective temperatures are 25 000 and 25 300 K, and $\log g = 5.4$ for both stars. Given the further similarity in periods, the large difference in the amplitude of the ellipsoidal variations is interesting: 17 (B) and 15 (V) mmag for KPD 0422+5421 (Koen et al. 1998) versus 4.5 (B) and 4.4 (V) mmag for HE 0218−3734. Morris (1985) provides the following approximation for the photometric amplitude due to ellipsoidal deformation:

$$\Delta m = 0.163 g(\tau, u_1) q R_{\rm p}^3 \sin^2 i / A^3,$$

$$g(\tau, u_1) = (\tau + 1)(15 + u_1)/(3 - u_1),$$

where q is the mass ratio $M_{\rm s}/M_{\rm p}$, $R_{\rm p}$ is the radius of the primary (i.e. ellipsoidal) star, A is the semimajor axis length, and the function g describes the influence of gravity darkening τ and limb darkening u_1. This equation can be combined with Kepler's third law to find

$$\Delta m = 2.189 \times 10^{-3} g(\tau, u_1) \frac{q R_{\rm p}^3 \sin^2 i}{(1 + q) M_{\rm p} P^2},$$

where P is the binary period (in days). The inclination angle $i > 84^\circ$ in KPD 0422+5421 (Orosz & Wade 1999), hence $\sin^2 i \approx 1$ in that system; to account for the factor ∼3.5 smaller amplitudes in HE 0218−3437, the inclination would have to be about $i = 30^\circ$. Alternatively, if the difference is to be explained solely in terms of the secondary star mass, then

$$\frac{q({\rm HE})}{1 + q({\rm HE})} \sim \frac{q({\rm KPD})}{3.5[1 + q({\rm KPD})]}$$

is required, leading to

$$q({\rm HE}) \sim \frac{q({\rm KPD})}{2.5 q({\rm KPD}) + 3.5}.$$

Orosz & Wade (1999) find a mass ratio close to unity for KPD 0422+5421; this would imply a mass ratio of 0.17 for HE 0218–3437, giving a secondary star mass of about 0.09 $M_\odot$. Given that the smallest WD mass discovered to date is 0.17 $M_\odot$ (Kilic et al. 2007), a small inclination angle is the more likely explanation. Of course, there is also the distinct possibility the difference in amplitudes is due to a combination of differences in inclinations, masses of the secondary star and properties of the hot subdwarfs.

3 LB 1516

LB 1516 was classified sdB by Heber (1986) who also determined $T_{\rm eff} = 23\,300$ K and $\log g = 5.4$. More recently, Edelmann (2003) found $T_{\rm eff} = 26\,100$ K and $\log g = 5.4$; both measurements place it in the instability region of the slowly pulsating sdB stars. It is a radial velocity variable; probably a binary star with a period in the range 9–27 d (Edelmann et al. 2005). Abundance analyses of various elements have been published by Edelmann, Heber & Napiwotzki (2001) and Chayer et al. (2006), and the chemical composition of LB 1516 does not appear unusual for an sdB star.

The combined optical photometry (see Table 1) and 2MASS photometry places the star amongst composite, rather than single, systems in the two-colour diagrams of Reed & Stiening (2004).

Table 4. The observing log for LB 1516.

Start HJD (2454700+)	$T_{\rm exp}$ (s) B	V	R_C	Run (h)	n
36.362 29	30	20–30		4.4	108, 104
37.238 97	30	25–35	25	8.2	188, 185, 178
38.230 57	30–45	25–30	25–45	7.2	145, 149, 101
39.306 63	30–40	25	25	3.7	84, 84, 81
40.231 80	25–30	20	20	8.3	234, 221, 230

Note. Much of the observing was done through thin cirrus, which required adjustment of the exposure time $T_{\rm exp}$. The number of useful measurements through each of the three filters is given in the last column (in the order B, V and R_C).

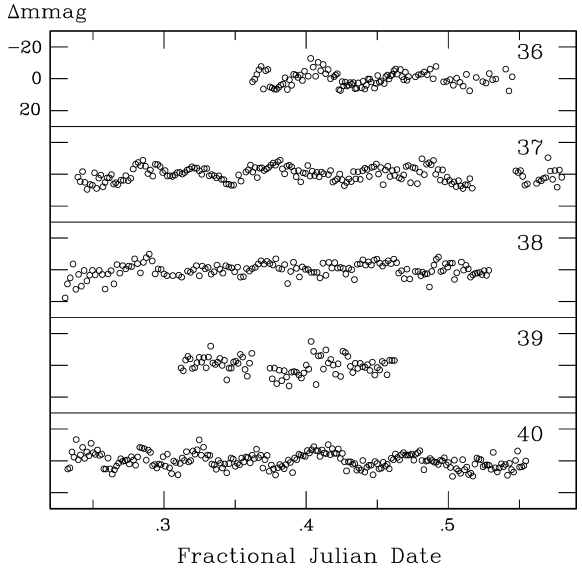

Figure 6. Differential light curves obtained in the V band for LB 1516. The vertical width of each panel is 0.06 mag. Panels are labelled with the last two digits of the Julian Day of observation.

3.1 Observations

All measurements were made with the STE4 CCD camera mounted on the 1.0-m telescope at the Sutherland site of the SAAO. The field of view of the camera on the telescope is ∼5 × 5 arcmin^2. Pre-binning of the images was performed throughout, giving a reasonable readout time of roughly 20 s. Observations were cycled through the B, V and R_C filters; Table 4 gives an observing log.

Photometric reductions were performed using an automated version of DOPHOT (Schechter et al. 1993). Both profile-fitted and aperture magnitudes were calculated, and the least noisy of the two for a given night was selected. Differential measurements with respect to two or three of the brightest stars in the field of view were calculated. A sample set of light curves (V) is plotted in Fig. 6.

3.2 Analysis

Pre-whitening the data by a second order polynomial removed variability with frequencies below about 3 d^{-1}. The remaining higher frequency content in the three data sets can be seen in Fig. 7. There is some residual power below 10 d^{-1}, particularly in the B and R bands. In the case of the blue filter, this can probably be ascribed to differential extinction, but in the case of the R filter this ought to play a lesser role, and we can offer no plausible explanation for the hump of power around 6 d^{-1}.

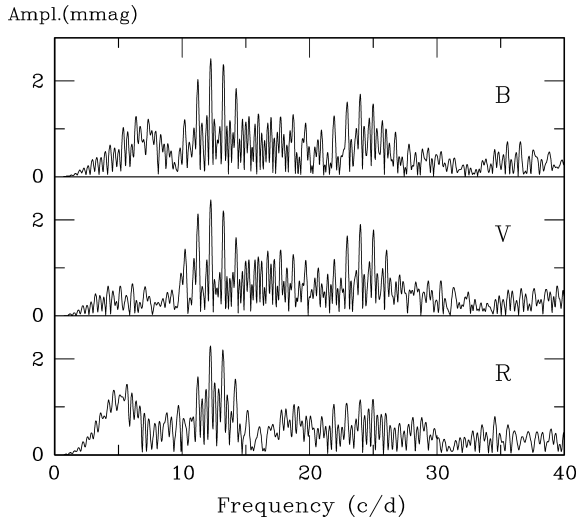

Figure 7. Amplitude spectra of the three sets of LB 1516 photometry.

Table 5. A complete inventory of LB 1516 amplitude spectrum peaks, obtained by successive pre-whitening in the range $0 < f < 40\,\mathrm{d}^{-1}$, for each of the three data sets.

Frequency (d^{-1})			Amplitude (mmag)		
B	*V*	R_C	*B*	*V*	R_C
12.24 (1)	12.25 (1)	12.22 (2)	2.4 (2)	2.4 (2)	2.2 (2)
		5.66 (3)			1.4 (2)
23.98 (2)	24.00 (1)	23.98 (3)	1.9 (2)	2.1 (2)	1.3 (2)
18.72 (2)	18.74 (2)	18.77 (3)	1.3 (2)	1.3 (2)	1.1 (2)
6.36 (2)			1.2 (2)		
		4.14 (4)			1.0 (2)
25.74 (2)	25.77 (2)	27.73 (4)	1.1 (2)	1.0 (2)	0.8 (2)
16.00 (3)	16.24 (3)		1.0 (2)	0.9 (2)	

Note. Figures in brackets are the uncertainties in the last quoted digit; these are formal errors, which could consistently underestimate the true errors.

Analyses of all the observations for a given filter were performed. Amplitude spectra were calculated over the range [0, 40] d^{-1}, and the frequency corresponding to the highest peak identified. This frequency was then pre-whitened from the data, and the process repeated. The results of several stages of pre-whitening are given in Table 5.

Inspection of the table shows excellent agreement between the four most prominent frequencies in the *V* data, and four corresponding frequencies in *B*. In the case of a fifth frequency, the difference is rather large (16.24 and 16.00 d^{-1}, respectively), and it is not certain that the variation is intrinsic to the star. The three largest amplitude modes in *V* and *B* are also observed in *R*. In the case of the fourth frequency ($f = 25.77$ in *V*), an alias ($f = 27.73$) may have been observed in *R*, although this appears questionable in view of results presented below.

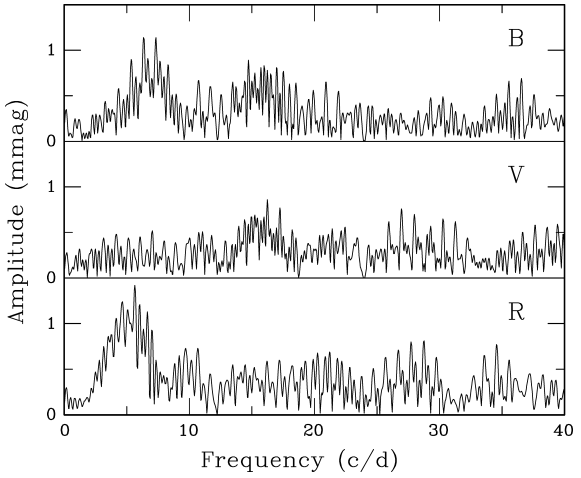

Figure 8. Amplitude spectra of three residual data sets for LB 1516, after pre-whitening by the frequencies listed in Table 6.

Simultaneous non-linear least squares fits of several sinusoids were next performed. Only frequencies showing good agreement between the different filters were included (four for *B* and *V*, three for *R*). Results are summarized in Table 6. Attention is drawn in particular to the facts that (i) for each of the frequencies, the variations seen in the different filters are in phase, and that (ii) the *V*-band amplitudes are *all* comparable to the corresponding *B*-band amplitudes.

Amplitude spectra of the three sets of residuals (i.e. the data left after removal of the Table 6 fits) are in Fig. 8. Focussing on the *R*-band spectrum, it appears unlikely that the 27.7 d^{-1} peak is an alias of the 25.7 d^{-1} frequency found in the *V* and *B* data.

4 CONCLUSIONS

We have shown two known sdB stars, HE 0218−3437 and LB 1516, to be variable. LB 1516 appears to be a typical slowly pulsating sdB star with several frequencies in the range 12 to 25 cycles d^{-1} (equivalent to periods in the range of about 1 to 2 h). The origin of the variability in HE 0218–3437 is not obvious: the temperature and gravity given in Table 1 place the star in the instability strip of slowly pulsating sdB (PG 1716) stars. The small amplitudes, and the lengths of the periods, are also consistent with this type of variability, as are the ratios of the amplitudes seen in the different filters. However, the apparently non-sinusoidal nature, and monoperiodicity, are features that have not been observed in any other variable of this type. It seems more likely that the star is in a binary system and that the variations are due to ellipsoidal distortion of the primary star.

Table 6. The results of simultaneously fitting several sinusoids to the data by a non-linear least squares method.

Frequency (d^{-1})			Amplitude (mmag)			Phase		
B	*V*	R_C	*B*	*V*	R_C	*B*	*V*	R_C
12.243 (9)	12.242 (8)	12.22 (1)	2.6 (2)	2.6 (2)	2.3 (2)	0.2 (2)	0.2 (1)	0.3 (2)
23.97 (1)	23.99 (1)	23.98 (2)	1.8 (2)	2.1 (2)	1.3 (2)	2.6 (2)	2.4 (2)	2.3 (4)
18.72 (2)	18.74 (1)	18.76 (3)	1.4 (2)	1.4 (2)	1.1 (2)	3.3 (3)	3.1 (2)	2.6 (5)
25.74 (2)	25.76 (2)		1.2 (2)	1.1 (2)		3.1 (3)	3.2 (3)	

Note. Fitting for each of the three data sets was carried out independently.

Time series spectroscopy of the star may provide further useful information.

It is also desirable to obtain photometry of HE 0218−3734 with a space-based, or a large-aperture terrestrial telescope, since observations with sufficient signal-to-noise ratio may allow any reflection effect to be identified. Furthermore, it may be possible to discriminate between gravity darkening and eclipses as explanations for the unequal photometric minima seen in Fig. 5.

ACKNOWLEDGMENTS

CK and DK acknowledge financial support for this project from the South African National Research Foundation. The authors thank Prof. Gilles Fontaine (University of Montreál) for very helpful input. CK thanks Dr Phil Massey (Lowell Observatory) for making available CCD reduction scripts, and for useful correspondence about these. DJF thanks Ralph Martin for technical help at Perth Observatory, and the Government of Western Australia for funding this research programme through a DEC grant.

REFERENCES

Altmann M., Edelmann H., de Boer K. S., 2004, A&A, 414, 181
Charpinet S., Fontaine G., Brassard P., Dorman B., 1996, ApJ, 471, L103
Charpinet S., Fontaine G., Brassard P., Chayer P., Green E. M., Randall S. K., 2007, Communications Asteroseismology, 150, 241
Charpinet S., Van Grootel V., Fontaine G., Brassard P., Green E. M., Chayer P., Randall S. K., 2008, A&A, 489, 377
Chayer P., Fontaine M., Fontaine G., Wesemael F., Dupuis J., 2006, Baltic Astron., 15, 131
Cleveland W. S., 1979, J. Am. Stat. Assoc., 74, 829
Cleveland W. S., Devlin S. J., 1988, J. Am. Stat. Assoc., 83, 596
Deeming T. J., 1975, Ap&SS, 36, 137
Edelmann H., 2003, PhD thesis, Univ. Erlangen-Nürnberg
Edelmann H., Heber U., Napiwotzki R., 2001, Astron. Nachr., 322, 401
Edelmann H., Heber U., Altmann M., Karl C., Lisker T., 2005, A&A, 442, 1023
Geier S., Nesslinger S., Heber U., Przbilla N., Napiwotzki R., Kudritzki R.-P., 2007, A&A, 464, 299
Geier S., Karl C., Edelmann H., Heber U., Napiwotzki R., 2008a, Mem. Soc. Astron. Ital., 79, 608
Geier S., Nesslinger S., Heber U., Randall S. K., Edelmann H., Green E. M., 2008b, A&A, 477, L13
Green E. M. et al., 2003, ApJ, 583, L31
Han Z., Podsiadlowski P., Maxted P. F. L., Marsh T. R., Ivanova N., 2002, MNRAS, 336, 449
Han Z., Podsiadlowski P., Maxted P. F. L., Marsh T. R., 2003, MNRAS, 341, 669
Heber U., 1986, A&A, 155, 33
Kilic M., Allende Prieto C., Brown W. R., KOester D., 2007, ApJ, 660, 1451
Kilkenny D., 2007, Communications Asteroseismology, 150, 234
Kilkenny D., Koen C., O'Donoghue D., Stobie R. S., 1997, MNRAS, 285, 640
Koen C., Orosz J. A., Wade R. A., 1998, MNRAS, 300, 695
Kurtz D. W., 1985, MNRAS, 213, 773
Landolt A. U., 2007, AJ, 133, 2502
Lutz R., Schuh S., Silvotti R., Bernabei S., Dreizler S., Stahn T., Húgelmeyer S. D., 2009, A&A, 496, 469
Luyten W. J., Anderson J. H., 1958, A Search for Faint Blue Stars. XII. The Far Southern Hemisphere. Univ. Minnesota, Minneapolis
Morris S. L., 1985, MNRAS, 295, 143
O'Donoghue D., 1995. Baltic Astron., 4, 519
Oreiro R., Ulla A., Pérez Hernández F., Rodriguez López C., MacDonald J., 2004, A&A, 418, 243
Orosz J. A., Wade R. A., 1999, MNRAS, 310, 773
Ortiz R., Malacarne M., Wilhelm R., Costa R. D. D., Rossi S., Maciel W. J., Costa A. F. M., 2007, AJ, 134, 1183
Reed M., Stiening R., 2004, PASP, 116, 506
Schechter P. L., Mateo M., Saha A., 1993, PASP, 105, 1342
Schuh S., Heber U., Dreizler S., O'Toole S., Green E., Fontaine G., 2006, A&A, 445, L31
Stark M. A., Wade R. A., 2003, AJ, 126, 1455
Van Grootel V., Charpinet S., Fontaine G., Brassard P., 2008a, A&A, 483, 875
Van Grootel V., Charpinet S., Fontaine G., Brassard P., Green E. M., Chayer P., Randall S. K., 2008b, A&A, 488, 685

This paper has been typeset from a TEX/LATEX file prepared by the author.